

# Optically Processed Broadband Microwave Imaging using a Spectral Hole Burning Medium as a Narrowband Image Sieve

Benjamin Braker, Youzhi Li, Friso Schlottau, Donghua Gu, and Kelvin Wagner  
University of Colorado, Boulder, CO 80309-0425  
braker.schlottau@colorado.edu

## Abstract

We present a 1-D broadband (4 GHz) microwave imager. The imager uses a Fourier optical beamformer to generate a squinted broadband image which is then spectrally resolved by burning a spatial distribution of spectral signals into a spectral hole burning material. These independent narrowband images may be read out, individually scaled to compensate for beam squint, and summed to form a broadband microwave image.

## 1 Introduction

This paper describes experimental 1-D broadband microwave image formation using a Fourier optical method that exceeds the capabilities of traditional RF analog or DSP techniques without the use of complex microwave receivers or supercomputer level digital processing. Such an image is useful in radio astronomy, signal surveillance, and other applications of passive microwave imaging. Traditional imaging techniques build images by scanning a given scene, but time varying objects or blinking sources require a staring imager to avoid missing a source while scanning another direction. Digital approaches to staring multibeam microwave imaging from antenna arrays require either unobtainable microwave analog-to-digital converters sampling the full RF bandwidth at each antenna element, or complex down-converting narrowband coherent receivers which process only a small fraction of the full RF bandwidth. The imaging system presented in this paper instead uses an optical Fourier processor, which allows rapid imaging without massive parallel digitization or RF receivers[1, 2]. In our approach, we correct for the beam squint inherent in broadband imaging by capturing independent images at each spectral frequency in a cryogenically-cooled spectral hole burning (SHB) crystal and then using a swept frequency laser to sequentially read out each

spectral image with a synchronously scanned zoom lens to compensate for the frequency dependent magnification of beam squint.

### 1.1 Beam Squint

Signals from broadband far-field sources arrive at a receiving antenna array with a time delay that varies linearly with the element position across the transverse array, as illustrated in Figure 1. For a given time delay, the phase scales with the frequency, and the spatial, linear time delay ramp results in a scaling of the images produced by spatial Fourier beam-forming. This phenomena occurs in broadband imaging and is called beam squint. Its compensation substantially increases the computational burden by requiring true-time-delay multiple beam-forming or frequency-channelized beam-forming. Real-time imaging using a wide bandwidth antenna array with a large number of elements is inevitably corrupted by beam squint and is beyond the capability of current or projected digital approaches.

### 1.2 Spectral Hole Burning

Spectral hole burning utilizes the inhomogeneously broadened absorption of two-level atoms doped into a cryogenically cooled crystal. Each atom absorbs a specific wavelength of light that is determined by the state of the surrounding crystal lattice. Lowering the temperature of the crystal reduces phonon broadening and decreases the homogeneous linewidth, which allows many thousands of spectrally resolvable absorbers at each resolvable spot in the crystal. Additional randomness in the structure of this crystal, such as the co-doping of a second ion, yields larger spreads in the distribution of these absorber center frequencies and can widen the crystal linewidth up to tens- or even hundreds- of GHz [3]. A strong laser can burn a spectral hole in the inhomogeneously

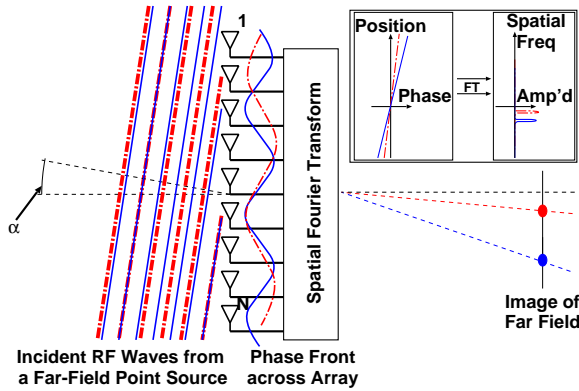


Figure 1: Beam squint in a Fourier beamformer. A far-field point source emitting at multiple spectral frequencies generates multiple plane waves, each of equal time delay, at the antenna array. The phase of these signals varies with frequency such that, when fed through the same spatial Fourier process, the perceived image is scaled with the frequency content.

broadened absorber profile, thereby addressing the crystal at a specific wavelength. This spectral selectivity of the SHB recording media allows parallel integration of the microwave images at each frequency while a long (10 ms) lifetime allows the slow sequential readout of the spectrally resolvable images. Our experiment uses the spectral absorption property as a hyperspectral color film, with a large number of selectable channels separated by MHz resolutions. Previous work in this area has concentrated on the spectral holographic properties of the crystal. Our experiment couples the spatial and spectral dimensions to create the spatial-spectral processing of a broadband imaging system. The image at each frequency persists within the crystal and is sequentially read out by a frequency scanned laser and synchronously magnified in proportion to the offset frequency to correct for beam squint.

## 2 Experimental Overview

In Figure 3 we have illustrated the transforms that generate an image from the electric field sampled by the antenna array. A far field point source generates transverse plane waves that impinge on the plane of the antenna array. A broadband RF signal may be written with  $r, t, M, \omega_m, c$ , and  $\theta$  representing the transverse spatial coordinate, time, the number of resolvable spectral frequencies, the narrowband RF frequency, the speed of light, and the angle of

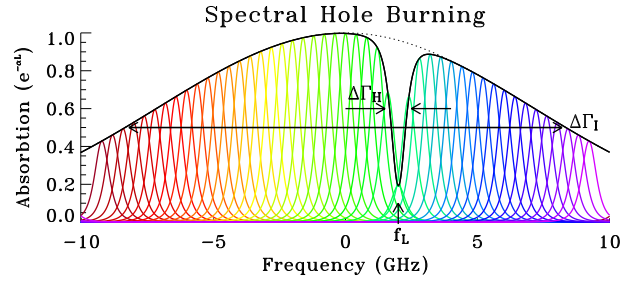


Figure 2: Spectral hole burning absorption profile. The inhomogeneously broadened spectrum of a spectral hole burning material combines a large number of spectrally overlapping homogeneously broadened absorbers to create a broad spectral absorption profile. A CW laser at  $f = f_L$  burns a hole in the spectral absorption profile of the crystal.

incidence, respectively.

$$E_f(r, t) = \sum_{m=1}^M \left( e^{-j\omega_m(t-r \sin \theta/c)} + e^{j\omega_m(t-r \sin \theta/c)} \right) \quad (1)$$

The field is received by an array of  $N$  antennas, each at a position  $r = r_k$ . This RF information is modulated onto an optical carrier,  $\omega_o$ , and placed into a topology preserving optical array with spatial coordinate  $x$ . Here, we neglect the complex conjugate term and write the result as follows.

$$E_o(x, t) = \sum_{m=1}^M e^{-j(\omega_o - \omega_m)t} \sum_{k=1}^N e^{-j\omega_m r_k \sin \theta/c + e_k} \delta(x - x_k) \quad (2)$$

This contains phase errors,  $e_k$ , due to errors in the RF length and thermal variations in the optical fiber length. If the optical carrier is uncohered, either by construction limitations or by temperature fluctuations in the optical phase between the fibers, then the phase error varies for each value of  $k$ , and optical energy is spread across the Fourier plane, as shown in Figure 3. When the optical array is cohered using a modified version of the redundant spacing calibration algorithm [4], such that  $e_k = 0$  for all  $k$ , it forms a peak in the Fourier plane and a single frequency modulation shifts the point source off axis, as we can see in the optical cross section.

The pictures in Figure 3 assume full modulation, but EOMs modulate only a small fraction of the input light. In the actual experiments, we expect a coherent superposition of the unmodulated peak with the modulated peak. After cohering, a lens of focal length  $F$  Fourier transforms the optical array.

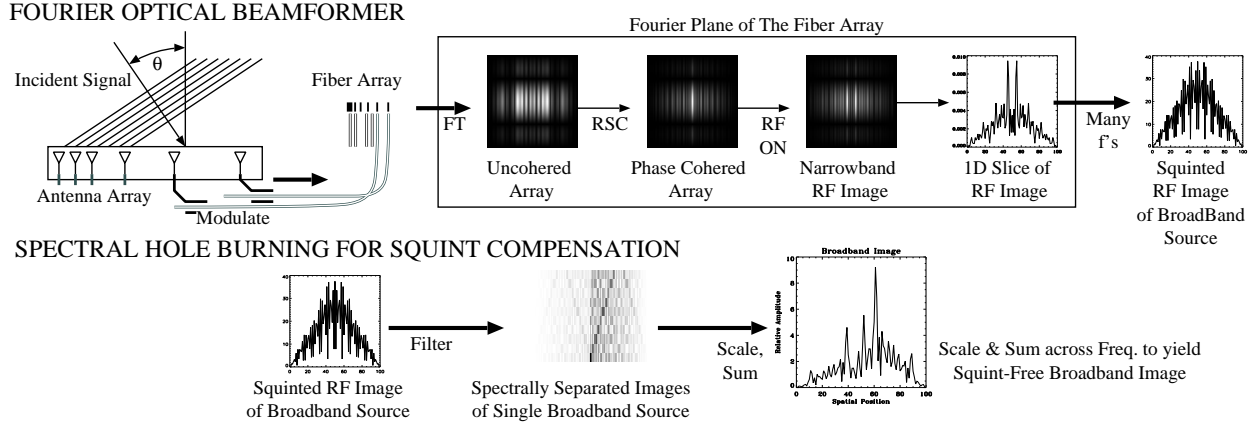


Figure 3: A functional cascade of the operations and simulated results of a broadband RF array imager. The RF wavefront impinges on the antenna array and is modulated onto the optical fiber array using EOMs. This topology preserving optical array is Fourier transformed and cohered such that when a signal is present, it forms 2 delta functions (DSB modulation) in the image plane. Broadband images have beam squint, so a spectral filter must select the narrowband image at each separate frequency. This allows for an independent scaling of each spectral image and then a summation across all frequencies to form a broadband image.

This forms the image of the far-field point source—limited only by the optical transfer function of the array,  $A(u) = \sum_{k=1}^N e^{-j2\pi x_k u / (\lambda F)}$ .

$$\begin{aligned}
 E_{FT}(u, t) &= \sum_{m=1}^M e^{-j(\omega_o - \omega_m)t} \mathcal{F} \left\{ \sum_{k=1}^N e^{j\omega_m r_k \sin \theta / c} \delta(x - x_k) \right\} \\
 &= \sum_{m=1}^M e^{-j(\omega_o - \omega_m)t} A \left( u - \omega_m \sin \theta \frac{\gamma F}{\omega_o} \right)
 \end{aligned} \tag{3}$$

Where the complex conjugate terms have been neglected and  $\gamma$  is the ratio of the RF array spacing to that of the optical array. We note that the spatial position scales with frequency and angle. If the signal is from a broadband point source, the image is spread radially, as illustrated in Figure 3. Narrowband spectrally filtered images are free from this beam squint. Each of these narrowband images can be re-scaled with frequency to correct for beam squint. The collection of spectral images provides a high resolution spectral analysis of each source in the microwave image, which can then be summed to form a single broadband image if spectral information is not needed.

converted into an array of optical signals with an array of amplifiers and EOMs. Piezoelectric stretchers dynamically correct variations in the optical path length to ensure relatively flat optical phase across the array. Polarization controllers align the polarization of the optical channels and allow for power balancing when used with a downstream polarizer. The optically modulated antenna array signals are applied to a topology-preserving scaled optical array and then spatially Fourier transformed by a lens to form the squinted far-field microwave image [1]. The squinted microwave images have a scale factor that varies linearly with microwave frequency. The system forms squinted microwave images within the SHB crystal such that each RF source produces a radially-scaled spectral image, each of which is recorded within the crystal as a spatial distribution of spectral holes. The system reads out the image at each frequency with a slow chirp of the laser. As the readout chirp scans across the frequency domain, it passes through the SHB crystal, which absorbs less light at spatial positions and spectral frequencies where the incident image burned absorption holes. Each spectral image is captured and digitally scaled to correct for beam squint.

## 2.1 Experimental Setup

Figure 4 illustrates the architecture of the microwave imager. First, a spatial sampling of the microwave signal(s) is collected with an antenna array and then

## 3 Results

To emulate the response from an object, a signal generator feeds the EOM array through a set of fixed

delay lines chosen with a maximum time delay across the array of 22 ns ( $1 \text{ ns} = \tau_{\min} = s_{\text{array}} \sin \theta / c$  per element spacing). This emulates a point source at  $17.5^\circ$  from the normal of an array with 1m spacing between elements. When injected with this emulated image, the imager forms a squinted image of the object. We then varied the frequency of the injected tone from 2-4 GHz and observed a shift in the spatial position of the image. The apparent position of the source varied with frequency, as shown in Figure 5, where we used a 7 element array with 16 resolvable points. This figure shows the average of 5 consecutive sweeps. The image aliases back into itself at the free spectral range of the array time delay and simultaneously shifts up and down because of the double sideband (DSB) nature of the modulators. The aliasing and DSB effects generate the interwoven diamond pattern, with a position shift with frequency that demonstrates beam squint.

## 4 Conclusion

We have described the experimental setup and have given preliminary results for a broadband microwave imager using Fourier optical processing. We showed the squinted image from a Fourier optical beamformer can be burned into an SHB crystal in order to read out and separate the narrowband image at each spectral bin for re-scaling and summation to form a squint-compensated broadband image.

## References

- [1] D. I. Voskresenski, A. I. Grinev, and E. N. Voronin, *Electrooptical Arrays*. NY: Springer-Verlag, 1989.
- [2] J. Bregman, F. Schlottau, K. Wagner, and J. L. L. Gouët, "Sparse array imaging and spectral analysis using spatial-spectral holography," in *Proc. IEEE Microwave Photonics (MWP 2003)*, (Budapest, Hungary), September 2003.
- [3] Y. Sun, C. W. Thiel, R. L. Cone, R. W. Equall, and R. L. Hutcheson, "Recent progress in developing new rare earth materials for hole burning and coherent transient applications," *J. Lumin.*, vol. 98, pp. 281–287, 2002.
- [4] P. M. Blanchard and A. H. G. et. al., "Coherent optical beam forming with passive millimeter-wave arrays," *Journal of Lightwave Technology*, vol. 17, pp. 418–425, 1999.

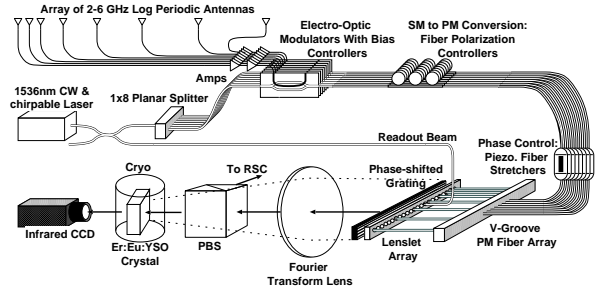


Figure 4: Experimental setup of the RF array imager. The antenna array receives the microwave signal and the EOMs modulate these signals onto an optical carrier such that an optical array captures an optical copy of the microwave array. The lens Fourier transforms the array to form the squinted image of the RF source(s) in the  $\text{Er}^{3+}:\text{Eu}^{3+}:\text{Y}_2\text{SiO}_5$  crystal. A chirped laser then generates a readout beam which forms a squinted narrowband image onto the infrared CCD at each spectral frequency bin.

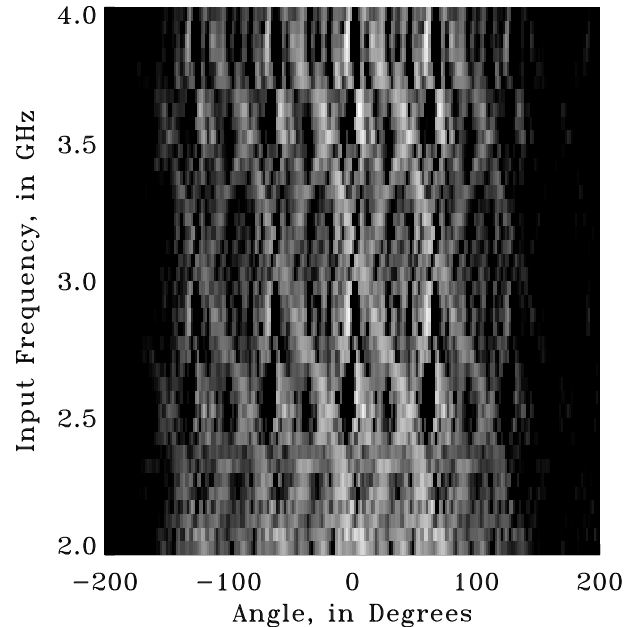


Figure 5: Experimental squinted image output from the Fourier optical beamformer. This shows a one dimensional image that varies as the input signal sweeps between 2 and 4 GHz. The horizontal axis represents spatial position while the vertical axis represents the frequency. We can see that as time progresses and the frequency of our image is shifted, the spatial position of its image is also shifted.